DESY 00-070
May 2000
ISSN 0418-9833

Measurement of elastic electroproduction of ϕ mesons at HERA

H1 Collaboration

Abstract

The elastic electroproduction of ϕ mesons is studied at HERA with the H1 detector for photon virtualities $1 < Q^2 < 15\ \mathrm{GeV}^2$ and hadronic centre of mass energies $40 < W < 130$ GeV. The Q^2 and t dependences of the cross section are extracted (t being the square of the four-momentum transfer to the target proton). When plotted as function of (Q^2 + M_V^2) and scaled by the appropriate SU(5) quark charge factor, the ϕ meson cross section agrees within errors with the cross sections of the vector mesons V = ρ, ω and J/ψ. A detailed analysis is performed of the ϕ meson polarisation state and the ratio of the production cross sections for longitudinally and transversely polarised ϕ mesons is determined. A small but significant violation of s-channel helicity conservation (SCHC) is observed.

To be submitted to *Phys. Lett. B.*

C. Adloff[33], V. Andreev[24], B. Andrieu[27], V. Arkadov[35], A. Astvatsatourov[35], I. Ayyaz[28], A. Babaev[23], J. Bähr[35], P. Baranov[24], E. Barrelet[28], W. Bartel[10], U. Bassler[28], P. Bate[21], A. Beglarian[34], O. Behnke[10], C. Beier[14], A. Belousov[24], T. Benisch[10], Ch. Berger[1], G. Bernardi[28], T. Berndt[14], J.C. Bizot[26], K. Borras[7], V. Boudry[27], W. Braunschweig[1], V. Brisson[26], H.-B. Bröker[2], D.P. Brown[21], W. Brückner[12], P. Bruel[27], D. Bruncko[16], J. Bürger[10], F.W. Büsser[11], A. Bunyatyan[12,34], H. Burkhardt[14], A. Burrage[18], G. Buschhorn[25], A.J. Campbell[10], J. Cao[26], T. Carli[25], S. Caron[1], E. Chabert[22], D. Clarke[5], B. Clerbaux[4], C. Collard[4], J.G. Contreras[7,41], J.A. Coughlan[5], M.-C. Cousinou[22], B.E. Cox[21], G. Cozzika[9], J. Cvach[29], J.B. Dainton[18], W.D. Dau[15], K. Daum[33,39], M. David[9,†], M. Davidsson[20], B. Delcourt[26], N. Delerue[22], R. Demirchyan[34], A. De Roeck[10,43], E.A. De Wolf[4], C. Diaconu[22], P. Dixon[19], V. Dodonov[12], J.D. Dowell[3], A. Droutskoi[23], C. Duprel[2], G. Eckerlin[10], D. Eckstein[35], V. Efremenko[23], S. Egli[32], R. Eichler[36], F. Eisele[13], E. Eisenhandler[19], M. Ellerbrock[13], E. Elsen[10], M. Erdmann[10,40,e], W. Erdmann[36], P.J.W. Faulkner[3], L. Favart[4], A. Fedotov[23], R. Felst[10], J. Ferencei[10], S. Ferron[27], M. Fleischer[10], G. Flügge[2], A. Fomenko[24], I. Foresti[37], J. Formánek[30], J.M. Foster[21], G. Franke[10], E. Gabathuler[18], K. Gabathuler[32], J. Garvey[3], J. Gassner[32], J. Gayler[10], R. Gerhards[10], S. Ghazaryan[34], L. Goerlich[6], N. Gogitidze[24], M. Goldberg[28], C. Goodwin[3], C. Grab[36], H. Grässler[2], T. Greenshaw[18], G. Grindhammer[25], T. Hadig[1], D. Haidt[10], L. Hajduk[6], W.J. Haynes[5], B. Heinemann[18], G. Heinzelmann[11], R.C.W. Henderson[17], S. Hengstmann[37], H. Henschel[35], R. Heremans[4], G. Herrera[7,41], I. Herynek[29], M. Hilgers[36], K.H. Hiller[35], J. Hladký[29], P. Höting[2], D. Hoffmann[10], W. Hoprich[12], R. Horisberger[32], S. Hurling[10], M. Ibbotson[21], Ç. İşsever[7], M. Jacquet[26], M. Jaffre[26], L. Janauschek[25], D.M. Jansen[12], X. Janssen[4], V. Jemanov[11], L. Jönsson[20], D.P. Johnson[4], M.A.S. Jones[18], H. Jung[20], H.K. Kästli[36], D. Kant[19], M. Kapichine[8], M. Karlsson[20], O. Karschnick[11], O. Kaufmann[13], M. Kausch[10], F. Keil[14], N. Keller[37], J. Kennedy[18], I.R. Kenyon[3], S. Kermiche[22], C. Kiesling[25], M. Klein[35], C. Kleinwort[10], G. Knies[10], B. Koblitz[25], S.D. Kolya[21], V. Korbel[10], P. Kostka[35], S.K. Kotelnikov[24], M.W. Krasny[28], H. Krehbiel[10], J. Kroseberg[37], D. Krücker[38], K. Krüger[10], A. Küpper[33], T. Kuhr[11], T. Kurča[35,16], R. Kutuev[12], W. Lachnit[10], R. Lahmann[10], D. Lamb[3], M.P.J. Landon[19], W. Lange[35], T. Laštovička[30], A. Lebedev[24], B. Leißner[1], R. Lemrani[10], V. Lendermann[7], S. Levonian[10], M. Lindstroem[20], E. Lobodzinska[10,6], B. Lobodzinski[6,10], N. Loktionova[24], V. Lubimov[23], S. Lüders[36], D. Lüke[7,10], L. Lytkin[12], N. Magnussen[33], H. Mahlke-Krüger[10], N. Malden[21], E. Malinovski[24], I. Malinovski[24], R. Maraček[25], P. Marage[4], J. Marks[13], R. Marshall[21], H.-U. Martyn[1], J. Martyniak[6], S.J. Maxfield[18], A. Mehta[18], K. Meier[14], P. Merkel[10], F. Metlica[12], H. Meyer[33], J. Meyer[10], P.-O. Meyer[2], S. Mikocki[6], D. Milstead[18], T. Mkrtchyan[34], R. Mohr[25], S. Mohrdieck[11], M.N. Mondragon[7], F. Moreau[27], A. Morozov[8], J.V. Morris[5], K. Müller[13], P. Murín[16,42], V. Nagovizin[23], B. Naroska[11], J. Naumann[7], Th. Naumann[35], G. Nellen[25], P.R. Newman[3], T.C. Nicholls[5], F. Niebergall[11], C. Niebuhr[10], O. Nix[14], G. Nowak[6], T. Nunnemann[12], J.E. Olsson[10], D. Ozerov[23], V. Panassik[8], C. Pascaud[26], G.D. Patel[18], E. Perez[9], J.P. Phillips[18], D. Pitzl[10], R. Pöschl[7], I. Potachnikova[12], B. Povh[12], K. Rabbertz[1], G. Rädel[9], J. Rauschenberger[11], P. Reimer[29], B. Reisert[25], D. Reyna[10], S. Riess[11], E. Rizvi[3], P. Robmann[37], R. Roosen[4], A. Rostovtsev[23], C. Royon[9], S. Rusakov[24], K. Rybicki[6], D.P.C. Sankey[5], J. Scheins[1], F.-P. Schilling[13], P. Schleper[13], D. Schmidt[33], D. Schmidt[10], L. Schoeffel[9], A. Schöning[36], T. Schörner[25], V. Schröder[10], H.-C. Schultz-Coulon[10], K. Sedlák[29], F. Sefkow[37], V. Shekelyan[25], I. Sheviakov[24], L.N. Shtarkov[24], G. Siegmon[15], P. Sievers[13], Y. Sirois[27], T. Sloan[17], P. Smirnov[24], V. Solochenko[23], Y. Soloviev[24], V. Spaskov[8],

A. Specka[27], H. Spitzer[11], R. Stamen[7], J. Steinhart[11], B. Stella[31], A. Stellberger[14], J. Stiewe[14], U. Straumann[37], W. Struczinski[2], M. Swart[14], M. Taševský[29], V. Tchernyshov[23], S. Tchetchelnitski[23], G. Thompson[19], P.D. Thompson[3], N. Tobien[10], D. Traynor[19], P. Truöl[37], G. Tsipolitis[36], J. Turnau[6], J.E. Turney[19], E. Tzamariudaki[25], S. Udluft[25], A. Usik[24], S. Valkár[30], A. Valkárová[30], C. Vallée[22], P. Van Mechelen[4], Y. Vazdik[24], S. von Dombrowski[37], K. Wacker[7], R. Wallny[37], T. Walter[37], B. Waugh[21], G. Weber[11], M. Weber[14], D. Wegener[7], A. Wegner[25], T. Wengler[13], M. Werner[13], G. White[17], S. Wiesand[33], T. Wilksen[10], M. Winde[35], G.-G. Winter[10], C. Wissing[7], M. Wobisch[2], H. Wollatz[10], E. Wünsch[10], A.C. Wyatt[21], J. Žáček[30], J. Zálešák[30], Z. Zhang[26], A. Zhokin[23], F. Zomer[26], J. Zsembery[9] and M. zur Nedden[10]

[1] *I. Physikalisches Institut der RWTH, Aachen, Germany*[a]
[2] *III. Physikalisches Institut der RWTH, Aachen, Germany*[a]
[3] *School of Physics and Space Research, University of Birmingham, Birmingham, UK*[b]
[4] *Inter-University Institute for High Energies ULB-VUB, Brussels; Universitaire Instelling Antwerpen, Wilrijk; Belgium*[c]
[5] *Rutherford Appleton Laboratory, Chilton, Didcot, UK*[b]
[6] *Institute for Nuclear Physics, Cracow, Poland*[d]
[7] *Institut für Physik, Universität Dortmund, Dortmund, Germany*[a]
[8] *Joint Institute for Nuclear Research, Dubna, Russia*
[9] *DSM/DAPNIA, CEA/Saclay, Gif-sur-Yvette, France*
[10] *DESY, Hamburg, Germany*[a]
[11] *II. Institut für Experimentalphysik, Universität Hamburg, Hamburg, Germany*[a]
[12] *Max-Planck-Institut für Kernphysik, Heidelberg, Germany*[a]
[13] *Physikalisches Institut, Universität Heidelberg, Heidelberg, Germany*[a]
[14] *Kirchhoff-Institut für Physik, Universität Heidelberg, Heidelberg, Germany*[a]
[15] *Institut für experimentelle und angewandte Physik, Universität Kiel, Kiel, Germany*[a]
[16] *Institute of Experimental Physics, Slovak Academy of Sciences, Košice, Slovak Republic*[e,f]
[17] *School of Physics and Chemistry, University of Lancaster, Lancaster, UK*[b]
[18] *Department of Physics, University of Liverpool, Liverpool, UK*[b]
[19] *Queen Mary and Westfield College, London, UK*[b]
[20] *Physics Department, University of Lund, Lund, Sweden*[g]
[21] *Department of Physics and Astronomy, University of Manchester, Manchester, UK*[b]
[22] *CPPM, CNRS/IN2P3 - Univ Mediterranee, Marseille - France*
[23] *Institute for Theoretical and Experimental Physics, Moscow, Russia*
[24] *Lebedev Physical Institute, Moscow, Russia*[e,h]
[25] *Max-Planck-Institut für Physik, München, Germany*[a]
[26] *LAL, Université de Paris-Sud, IN2P3-CNRS, Orsay, France*
[27] *LPNHE, École Polytechnique, IN2P3-CNRS, Palaiseau, France*
[28] *LPNHE, Universités Paris VI and VII, IN2P3-CNRS, Paris, France*
[29] *Institute of Physics, Academy of Sciences of the Czech Republic, Praha, Czech Republic*[e,i]
[30] *Faculty of Mathematics and Physics, Charles University, Praha, Czech Republic*[e,i]
[31] *INFN Roma 1 and Dipartimento di Fisica, Università Roma 3, Roma, Italy*
[32] *Paul Scherrer Institut, Villigen, Switzerland*
[33] *Fachbereich Physik, Bergische Universität Gesamthochschule Wuppertal, Wuppertal, Germany*[a]

[34] *Yerevan Physics Institute, Yerevan, Armenia*
[35] *DESY, Zeuthen, Germany*[a]
[36] *Institut für Teilchenphysik, ETH, Zürich, Switzerland*[j]
[37] *Physik-Institut der Universität Zürich, Zürich, Switzerland*[j]
[38] *Present address: Institut für Physik, Humboldt-Universität, Berlin, Germany*
[39] *Also at Rechenzentrum, Bergische Universität Gesamthochschule Wuppertal, Wuppertal, Germany*
[40] *Also at Institut für Experimentelle Kernphysik, Universität Karlsruhe, Karlsruhe, Germany*
[41] *Also at Dept. Fis. Ap. CINVESTAV, Mérida, Yucatán, México*[k]
[42] *Also at University of P.J. Šafárik, Košice, Slovak Republic*
[43] *Also at CERN, Geneva, Switzerland*
† *Deceased*

[a] *Supported by the Bundesministerium für Bildung, Wissenschaft, Forschung und Technologie, FRG, under contract numbers 7AC17P, 7AC47P, 7DO55P, 7HH17I, 7HH27P, 7HD17P, 7HD27P, 7KI17I, 6MP17I and 7WT87P*
[b] *Supported by the UK Particle Physics and Astronomy Research Council, and formerly by the UK Science and Engineering Research Council*
[c] *Supported by FNRS-FWO, IISN-IIKW*
[d] *Partially Supported by the Polish State Committee for Scientific Research, grant No. 2P0310318 and SPUB/DESY/P-03/DZ 1/99*
[e] *Supported by the Deutsche Forschungsgemeinschaft*
[f] *Supported by VEGA SR grant no. 2/5167/98*
[g] *Supported by the Swedish Natural Science Research Council*
[h] *Supported by Russian Foundation for Basic Research grant no. 96-02-00019*
[i] *Supported by GA AVČR grant number no. A1010821*
[j] *Supported by the Swiss National Science Foundation*
[k] *Supported by CONACyT*

1 Introduction

Vector meson production in lepton-proton collisions is a powerful probe to investigate the nature of diffraction. At HERA, because of the wide kinematic ranges in the photon virtuality, Q^2, and in the hadronic centre of mass energy, W, the details of the production mechanism can be studied. It is also possible to select different vector mesons, allowing the cross section for different quark types to be studied. Recent measurements of ρ meson electroproduction [1, 2] for high Q^2 values ($Q^2 \gtrsim 10$ GeV^2) and of J/ψ meson photo– and electroproduction [2–5] show a strong energy dependence of the $\gamma^\star p \to Vp$ cross sections. This behaviour indicates that the mass of the c quark or a high Q^2 value provides a hard scale in the interaction, and we study the elastic cross sections as a function of the scale ($Q^2 + M_V^2$), where M_V is the mass of the vector meson.

This paper presents a measurement of elastic ϕ meson electroproduction

$$e^+ + p \to e^+ + \phi + p \ ; \ \phi \to K^+ + K^-, \tag{1}$$

in the Q^2 range from 1 to 15 GeV^2, and in the W range from 40 to 130 GeV. The data were obtained with the H1 detector in two running periods when the HERA collider was operated with 820 GeV protons and 27.5 GeV positrons. A low Q^2 data set ($1 < Q^2 < 5$ GeV^2) with integrated luminosity of 125 nb^{-1} was obtained from a special run in 1995, with the ep interaction vertex shifted by 70 cm in the outgoing proton beam direction. This results in a higher acceptance for low Q^2 production. A larger sample of integrated luminosity of 3pb^{-1} with $2.5 < Q^2 < 15$ GeV^2 was obtained in 1996 under normal running conditions. The present measurements provide detailed new information in the region $1 \lesssim Q^2 \lesssim 6$ GeV^2 and they increase the precision of the H1 measurement of ϕ electroproduction with $Q^2 > 6$ GeV^2, which was first performed using data collected in 1994 [6]. They are compared to results of the ZEUS experiment in photoproduction [7] and at $Q^2 > 7$ GeV^2 [8]. The elastic ϕ meson cross section is also compared to elastic ρ [1,2,9], ω [10], J/ψ [2–5] and Υ [11,12] meson production results from H1 and ZEUS.

The event selection and the K^+K^- mass distribution is presented in section 2. In section 3, the elastic ϕ cross section is presented as a function of Q^2 and W. In order to minimise the uncertainties, the cross section is measured as a ratio to elastic ρ production, and the absolute elastic ϕ cross section is then extracted using the results for ρ production from [1]. A compilation of the ρ, ω, ϕ, J/ψ, and Υ cross sections is presented as a function of (Q^2 + M_V^2). The t dependence of the elastic ϕ cross section is analysed in section 4. A detailed analysis of the photon and ϕ meson polarisations is performed in section 5 and the 15 spin density matrix elements are extracted. The ratio R of the longitudinal to transverse ϕ cross sections is obtained as a function of Q^2. A compilation of the measurements of R for elastic ρ, ϕ and J/ψ meson production is presented as a function of Q^2/M_V^2.

The present analysis uses to a large extent the techniques described in the H1 publication on elastic ρ production [1].

2 Data selection

Elastic ϕ electroproduction events are selected on the basis of their topology in the H1 detector[1]. They must have a positron candidate and two oppositely charged hadron candidates, originating from a vertex situated in the nominal e^+p interaction region, with K^+K^- invariant mass in the range from 1.00 to 1.04 GeV. The scattered positron is identified as an electromagnetic cluster of energy larger than 15 GeV detected in the H1 backward electromagnetic calorimeter SPACAL [14][2]. The two hadron candidates are recognised as tracks of opposite signs, with a momentum transverse to the beam direction larger than 100 MeV, reconstructed in the H1 central tracking detector with a polar angle in the range from 20° to 160°. The vertex must lie within 30 cm along the beam axis from the nominal interaction point. The nature of the hadrons is not explicitly identified. Their charge and momentum are measured in the central part of the detector by means of a uniform 1.15 T magnetic field. No other activity must be observed in the detector since the scattered proton remains in the beam pipe and is not detected because of the small momentum transfer to the target in diffractive interactions. Events were therefore rejected if there were signals in the forward part of the detector (forward muon and forward proton tagger detectors) and if there were clusters in the liquid argon calorimeter with an energy above 0.5 GeV not associated with the hadron candidates. To reduce effects of QED radiative corrections, the selected events have to satisfy $\sum_{e,h}(E - p_z) > 45$ GeV.

The Q^2 variable is reconstructed from the incident electron beam energy and the polar angles of the positron and of the ϕ meson candidates (double angle method [15]). The W variable is reconstructed using in addition the energy and the longitudinal momentum of the ϕ meson candidate.

The variable t is the square of the four-momentum transfer to the target proton. At HERA energies, to a very good precision, the absolute value of t is equal to the square of the transverse momentum of the outgoing proton. The latter is computed, under the assumption that the selected event corresponds to reaction (1), as the square of the vector sum of the transverse momenta of the ϕ meson candidate and of the scattered positron. Events with $|t| < 0.5$ GeV^2 are selected in order to reduce the remaining production of proton dissociation events which have a flatter t distribution, and to suppress the production of hadron systems of which the ϕ is only part and in which the remaining particles were not detected.

The distribution of m_{KK}, the two particle invariant mass computed under the assumption that the hadron candidates are kaons, is presented in Fig. 1a and Fig. 1b for $m_{KK} < 1.12$ GeV and for $m_{KK} < 2.00$ GeV, respectively. A clear ϕ signal is observed in the data, with 424 events in the range $1.00 < m_{KK} < 1.04$ GeV.

The main backgrounds to reaction (1) are due to diffractive ϕ events in which the proton is excited into a system of higher mass which subsequently dissociates, and to the elastic production of ρ and ω vector mesons. The other backgrounds (other ϕ decay channels, higher mass resonances or non resonant production) are estimated to be less than a few percent. The fraction of proton dissociation background is assumed to be the same for ϕ as for ρ meson production

[1] A detailed description of the H1 detector can be found in [13].

[2] H1 uses a right-handed coordinate system with the z axis taken along the beam direction, the $+z$ direction being that of the outgoing proton beam. The x axis points towards the centre of the HERA ring.

and is taken to be 11$\pm$5 % as in [1]. The background due to ρ and ω production is estimated using the DIFFVM simulation [16]. The DIFFVM Monte Carlo simulation program is based on Regge theory and on the vector meson dominance model. The ρ and ω backgrounds are normalised to the $m_{\pi\pi}$ distribution observed in the data, where $m_{\pi\pi}$ is the invariant mass computed under the pion hypothesis for the hadron candidates. This is shown in Fig. 1c after the ϕ signal has been removed by selecting $m_{KK} > 1.04$ GeV. The background under the ϕ peak from ρ and ω meson production is Q^2 dependent and varies from 15 % to 4 %. For the full sample ($2.5 < Q^2 < 15\ \mathrm{GeV}^2$) this background is found to be 9$\pm$5 %.

The data are corrected for acceptances, efficiencies and detector resolution effects using the DIFFVM Monte Carlo simulation. The response of the H1 detector is fully simulated.

3 Elastic cross section

The elastic ϕ meson production cross section is obtained by first measuring the ratio of the ϕ to ρ cross sections and then using the ρ cross sections which were precisely measured as described in [1]. In the ratio, several uncertainties cancel, most notably the luminosity uncertainty, the contribution of the proton dissociation background and the trigger efficiency, which is very similar for both data samples since it is mostly based on the positron detection in the SPACAL. The remaining corrections account for the mass selection range and the differences in acceptances and t distribution. The correction for the accepted mass range ($0.6 < m_{\pi\pi} < 1.1$ GeV) in the ρ sample is $1.16 \pm 0.02\ ^{+0.05}_{-0.00}$ [1]; the correction for the mass range ($1.00 < m_{KK} < 1.04$ GeV) in the ϕ sample is estimated to be 1.03 ± 0.01 using the DIFFVM simulation. In both samples, hadron tracks must be detected in the central tracker with $20^\circ < \theta < 160^\circ$. Differences in the acceptances for the two samples, due to the different decay hadron and vector meson masses, are estimated as a function of Q^2, W and t using the DIFFVM simulations for ρ and ϕ production. Differences in the detector efficiency for pions and kaons are taken into account in the detector simulation. Finally the correction for events with $|t| > 0.5\ \mathrm{GeV}^2$ in the ρ and ϕ samples is estimated by assuming an exponentially falling $|t|$ distribution, using recent measurements for the slope parameter of the exponential [1, 2, 6–8]. The correction factor on the ϕ/ρ cross section ratio is 1.03 ± 0.02, independent of Q^2. The branching ratios of 0.49 and 1.0 were used for the decays $\phi \to K^+K^-$ and $\rho \to \pi^+\pi^-$ respectively.

Systematic errors on the measurement of the cross section ratio are estimated by varying all corrections within the errors. In addition, in both the ρ and ϕ simulations the cross section dependence on Q^2, W, t and the vector meson angular decay distributions were varied by amounts allowed by the present and most recent measurements [1, 2, 6–8].

The Q^2 dependence of the ϕ to ρ elastic cross section ratio is presented in Fig. 2 together with previous H1 [6] and ZEUS [7, 8] results. The values of the ratio are given in Table 1. The present measurements confirm the significant rise of the cross section ratio with Q^2. As Q^2 increases, the HERA cross section ratios approach the value $2/9$ expected from quark charge counting and SU(5). It should be noted that calculations based on perturbative QCD predict that the cross section ratio should exceed this value at very large Q^2 [17]. The W dependence of the ϕ to ρ elastic cross section ratio is measured in the range $40 < \mathrm{W} < 130$ GeV and is observed to be constant, within the experimental uncertainties.

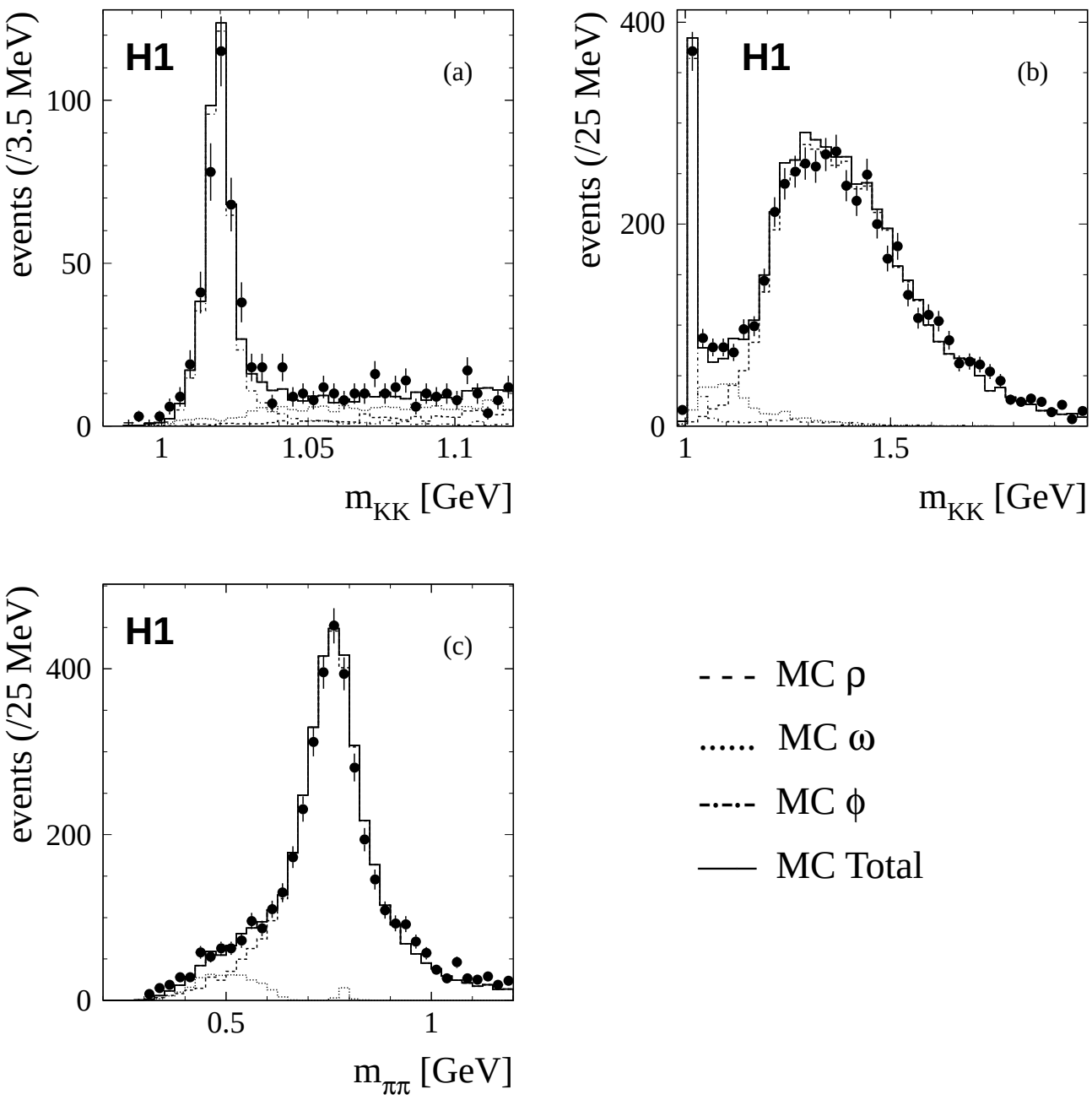

Figure 1: (a) and (b): distribution of m_{KK} for $m_{KK} < 1.12$ GeV and $m_{KK} < 2.00$ GeV, respectively; (c) distribution of $m_{\pi\pi}$ after removing the ϕ signal ($m_{KK} < 1.04$ GeV). The points represent the data and the full lines the prediction of a simulation, which includes contributions from elastic ρ (dashed lines), ω (dotted lines) and ϕ (dash-dotted lines) meson production. The errors on the data points are statistical only.

To extract the $\gamma^\star p \to \phi p$ cross section, the measurement of the ϕ/ρ cross section ratio is multiplied by the $\gamma^\star p \to \rho p$ cross section calculated from the fit in [1]. The values are given in Table 1. The systematic errors on the ϕ cross section measurement include the systematic errors on the ratio of ϕ to ρ cross sections, as well as an 8.4 % contribution coming from the parametrisation error in the fit of the ρ cross section (see [1]), added in quadrature.

In Fig. 3, the cross section for the elastic production of ϕ mesons (full squares) is presented together with other vector mesons V and for various values of Q^2, as a function of the variable (Q^2 + M_V^2). The data in Fig. 3 compile the HERA measurements [1–12] of the $\gamma^\star p \to Vp$ cross sections (see also [18]). The cross sections were scaled by SU(5) factors, according to the quark charge content of the vector meson, which amount to 1 for the ρ, 9 for the ω, 9/2 for the ϕ, 9/8 for the J/ψ and 9/2 for the Υ meson. The cross sections are measured at W = 75 GeV, or are moved to that value according to the parametrisation $\sigma \propto W^\delta$, using the δ value measured by the corresponding experiment. The ZEUS ρ and ϕ cross sections were corrected ($\lesssim$ 7 %) for the unmeasured signal with $|t| > 0.5$ (or 0.6) GeV^2 by assuming a simple exponential fall of $\mathrm{d}\sigma/dt \propto e^{bt}$. In this procedure the observed Q^2 dependence of the b slope was taken into account.

Within the experimental errors, the total cross sections for vector meson production, including the SU(5) normalisation factors, appear to lie on a universal curve when plotted as a function of the scale $(Q^2 + M_V^2)$, except possibly for the Υ photoproduction[3]. A fit performed on the H1 and ZEUS ρ data using the parametrisation $\sigma = a_1(Q^2 + M_V^2 + a_2)^{a_3}$, with a_1 = 10689 $\pm$ 165 nb, a_2 = 0.42 $\pm$ 0.09 GeV^2 and a_3 = – 2.37 $\pm$ 0.10 (χ^2/ndf = 0.67) is shown as the curve in Fig. 3. The ratio of the ω, ϕ and J/ψ cross sections to this parametrisation is presented in the insert of Fig. 3. Note that the universal $(Q^2 + M_V^2)$ dependence is for the total cross section measurements only. The separate behaviour of the longitudinal and transverse cross sections is described in ref. [18].

Q^2 (GeV^2)	$\sigma(\phi)/\sigma(\rho)$	$\sigma(\gamma^\star p \to \phi p)$ (nb)
1.3	$0.132 \pm 0.027 \pm 0.008$	$220 \pm 45 \pm 24$
2.22	$0.140 \pm 0.011\ ^{+0.009}_{-0.011}$	$96.3 \pm 7.6 \pm 10.6$
2.73	$0.159 \pm 0.015\ ^{+0.012}_{-0.015}$	$75.3 \pm 7.1 \pm 8.3$
3.44	$0.175 \pm 0.016\ ^{+0.012}_{-0.015}$	$53.7 \pm 4.9 \pm 5.9$
4.82	$0.197 \pm 0.019\ ^{+0.013}_{-0.016}$	$31.3 \pm 3.0 \pm 3.4$
7.53	$0.208 \pm 0.025\ ^{+0.013}_{-0.017}$	$13.3 \pm 1.6 \pm 1.5$
12.1	$0.207 \pm 0.046\ ^{+0.013}_{-0.017}$	$4.9 \pm 1.1 \pm 0.5$

Table 1: Ratio of the cross sections for elastic ϕ and ρ production and the elastic ϕ meson cross sections $\sigma(\gamma^\star p \to \phi p)$, for seven Q^2 values. The cross sections are given for W = 75 GeV. The first error represents the statistical error and the second the systematic error.

[3]The cross sections $\sigma(\gamma p \to \Upsilon(1S)p)$ measured by H1 and ZEUS at W = 143 and 120 GeV respectively [11, 12], were moved to the value W = 75 GeV using the parametrisation $\sigma \propto W^\delta$, with δ = 1.7. This high value of the parameter δ comes from the prediction of [19]. Note that if the value δ = 0.8 is used (a value measured in case of J/ψ photoproduction), the cross sections increase by a factor 1.5 for ZEUS and 1.8 for H1.

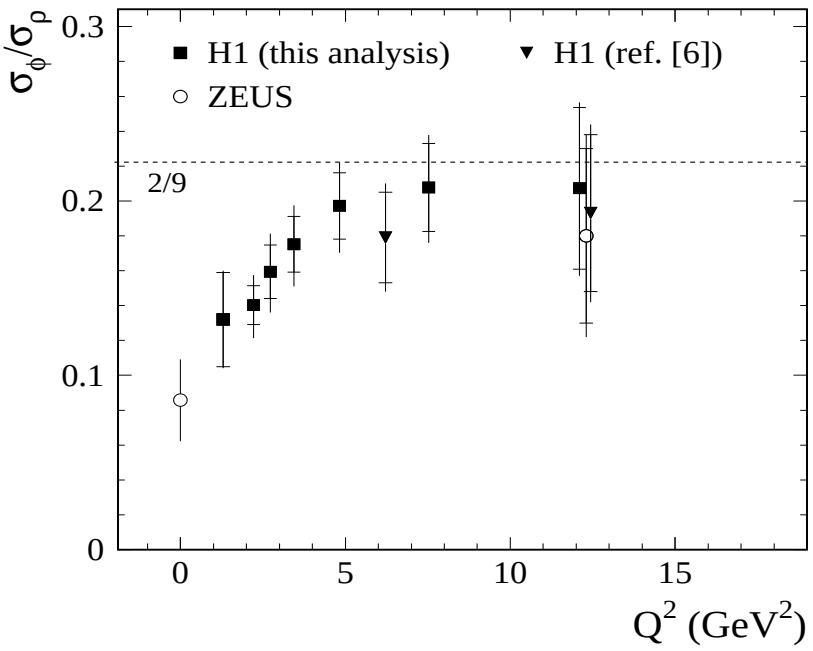

Figure 2: Ratio of the cross sections for elastic ϕ and ρ production, as a function of Q^2, together with previous H1 [6] and ZEUS [7,8] measurements. The inner error bars are statistical and the full error bars include the systematic errors added in quadrature. The dashed line corresponds to the ratio $2/9$.

4 Dependence on *t*

In this section and the following one, the elastic ϕ meson production is studied using the ϕ sample defined above, with the additional selection: the centre of gravity of the scattered positron cluster was required to lie outside the innermost part of the SPACAL calorimeter $-16 < x < 8$ cm and $-8 < y < 16$ cm in order to obtain good (> 95 %) and uniform trigger efficiency. The number of elastic ϕ candidates is then reduced to 221 events for $2.5 < Q^2 < 15$ GeV^2.

The measured $|t|$ dependence is shown in Fig. 4 and the characteristic falling exponential distribution is observed. To take into account the contribution of different backgrounds, the $|t|$ distribution is fitted by the sum of three exponentials corresponding to the elastic ϕ component, the diffractive ϕ component with proton dissociation and the ω and ρ production. The elastic ϕ component is fitted with a free normalisation and a free slope parameter b, whereas the other contributions are fixed to their calculated values. The contribution of diffractive ϕ events with proton dissociation of $11 \pm 5\,\%$ of the elastic signal and a slope parameter of 2.5 ± 1.0 GeV^{-2}, was taken from [1]. The ω and ρ background contributions, amounting to $9 \pm 5\,\%$ of the signal (see section 2), have an effective slope parameter b = 2.9 $\pm$ 0.6 GeV^{-2}, computed using the DIFFVM simulation.

The fitted exponential slope parameter for elastic ϕ events is found to be b =5.8$\pm$0.5 (stat.) $\pm$0.6 (syst.) GeV^{-2}, for an average Q^2 value of 4.5 GeV^2 and $\langle W \rangle$=75 GeV. The systematic

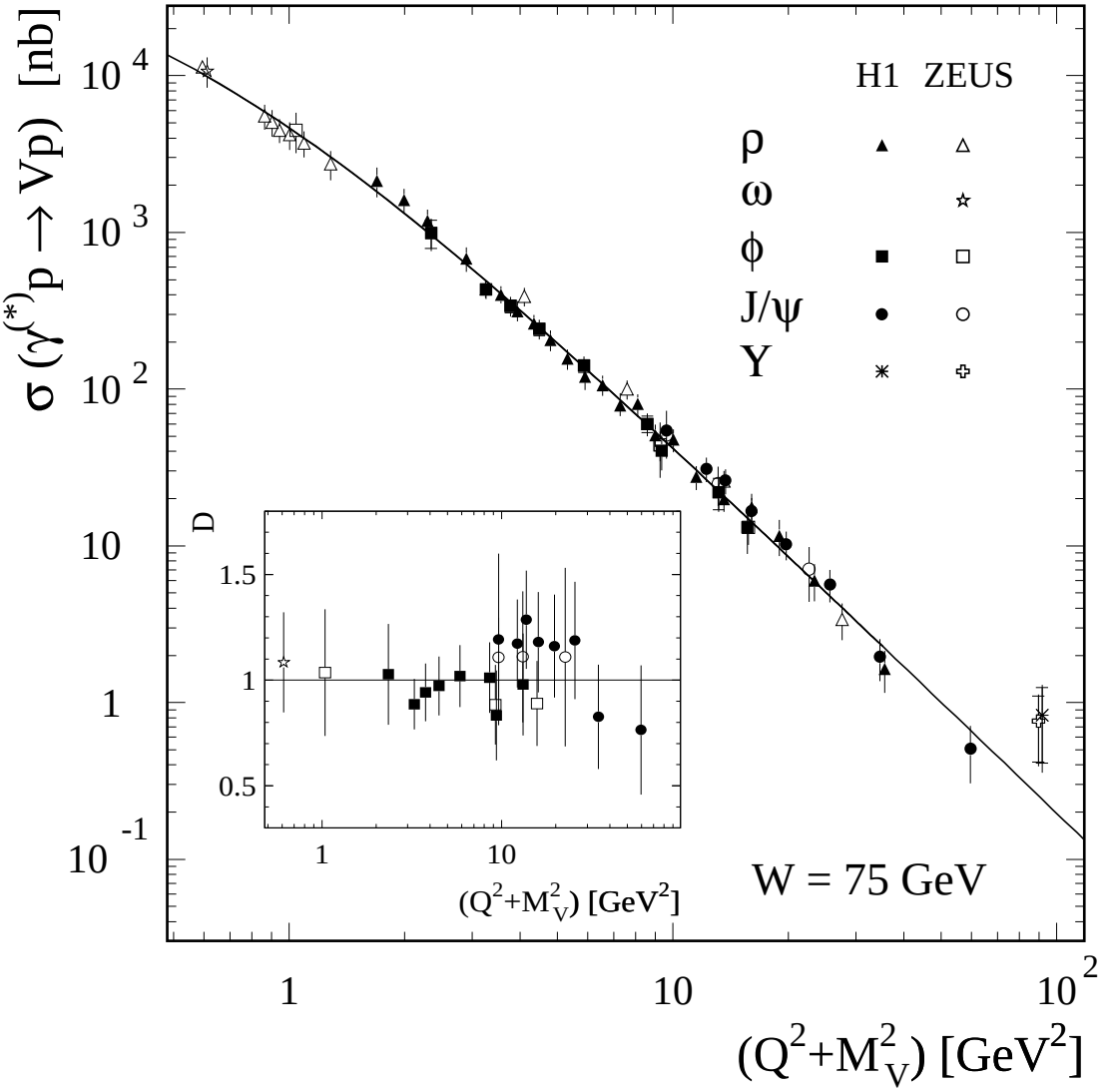

Figure 3: H1 and ZEUS measurements [1–12] of the total cross sections $\sigma(\gamma^\star p \to Vp)$ as a function of $(Q^2 + M_V^2)$ for elastic ρ, ω, ϕ, J/ψ and Υ meson production, at the fixed value W = 75 GeV. The cross sections were scaled by SU(5) factors, according to the quark charge content of the vector meson. For the error bars statistical and systematic errors have been added in quadrature. The curve corresponds to a fit to the H1 and ZEUS ρ data, and the ratio D of the scaled ω, ϕ and J/ψ cross sections to this parametrisation is presented in the insert.

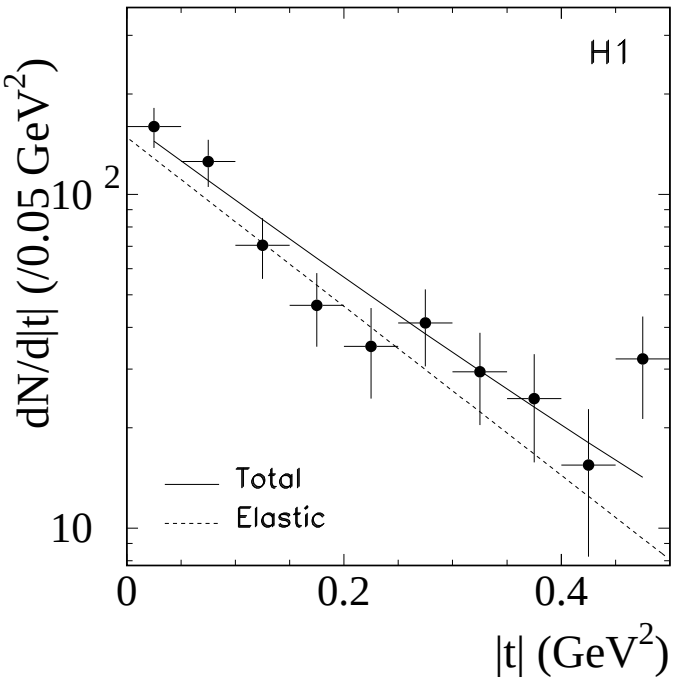

Figure 4: Corrected t distributions for elastic ϕ meson production, in the range $2.5 < Q^2 < 15\ \mathrm{GeV}^2$. The full curve presents the result of the fit to the sum of three exponentials (see text), the dotted line showing the elastic contribution. The errors on the data points are statistical only.

error is computed by varying the amounts of the background contributions and their slopes within the quoted errors, and by varying the binning and the limits of the fit. The effect of the QED radiative corrections on the b measurement is estimated using the simulation DIFFVM including a HERACLES [20] interface, and is found to decrease the value of the b measurement by 0.13 GeV^{-2} (the b value given above is not corrected for this effect). This result can be compared with other measurements, $b = 7.3 \pm 1.0 \pm 0.8\ \mathrm{GeV}^{-2}$ in photoproduction [7] and $b = 5.2 \pm 1.6 \pm 1.0\ \mathrm{GeV}^{-2}$ for $\langle Q^2 \rangle$ = 10 GeV^2 [6]. The data are consistent with a decrease of the slope parameter as Q^2 increases; this would be expected from the decrease of the transverse size of the virtual photon.

The value of the b slope parameter is in agreement within the errors with the one obtained in elastic ρ meson production: b = 5.5 $\pm$ 0.5 (stat.) $^{+0.5}_{-0.2}$ (syst.) GeV^{-2}, at Q^2 = 4.8 GeV^2 [1].

5 Polarisation studies

The study of the angular distributions of the production and decay of the ϕ meson provides information on the photon and ϕ meson polarisation states. In the helicity system [21], three angles are defined as follows. The angle Φ, defined in the hadronic centre of mass system (cms), is the azimuthal angle between the electron scattering plane and the plane containing

the ϕ meson and the scattered proton. The ϕ meson decay is described by the polar angle θ and the azimuthal angle φ of the positive kaon in the K^+K^- rest frame, with the quantisation axis taken as the direction opposite to that of the outgoing proton in the hadronic cms (the so called helicity frame). Details of the kinematics and the mathematical formalism can be found in [21] and [1]. The normalised angular decay distribution $F(\cos\theta,\ \varphi,\ \Phi)$ is expressed as a function of 15 spin density matrix elements corresponding to different bilinear combinations of the helicity amplitudes $T_{\lambda_\phi,\lambda_\gamma}$, where λ_ϕ and λ_γ are the helicities of the ϕ meson and of the photon, respectively. In the case of s-channel helicity conservation (SCHC), the helicities of the ϕ meson and the photon are equal, only the amplitudes T_{00}, T_{11}, and T_{-1-1} are different from zero and 10 of the 15 matrix elements are zero.

The matrix elements are measured using projections of the decay angular distribution onto orthogonal trigonometric functions of the angles θ, φ and Φ [21]. The results are presented in Fig. 5 in two Q^2 bins: $2.5 < Q^2 < 4.5\ \mathrm{GeV}^2$ and $4.5 < Q^2 < 15\ \mathrm{GeV}^2$. In Fig. 5, the results are not corrected for the small effects due to proton dissociation, ω and ρ production backgrounds and radiative effects.

The matrix elements generally follow the SCHC predictions, except for the elements r^1_{00} and r^5_{00}, which may indicate a small violation of SCHC. The matrix element r^5_{00} is proportional to the product $T^*_{00}T_{01}$ of helicity amplitudes, the dominant SCHC violating amplitude being T_{01} (λ_ϕ = 0 and λ_γ = 1).

Predictions from recent models based on perturbative QCD [22–24] are compared to the measurement of the 15 matrix elements. The models are expected to be valid at high Q^2 (providing a scale for the perturbative expansion) and at high energy: $W^2 \gg Q^2 \gg \Lambda^2_{\mathrm{QCD}}$. The ϕ meson production is factorised, in the proton rest frame, into three parts involving different time scales: the fluctuation of the photon into a $q\bar{q}$ state, at a large distance from the target, the hard scattering of the $q\bar{q}$ pair with the proton, modelled as two-gluon exchange, and the $q\bar{q}$ pair recombination into a ϕ meson wave. The amplitudes are computed separately for the different helicities of the photon and the ϕ meson. In models [23, 24], the gluon density in the proton is used for the computation of the hard scattering amplitude. Differences between the models are related to the way of introducing quark off-shellness and Fermi motion. All models describe the data relatively well, predicting in particular a non-zero value for the r^5_{00} matrix element (see Fig. 5). The model [23] gives a poorer description of the Q^2 dependence of the r^{04}_{00}, r^1_{1-1} and Im r^2_{1-1} matrix elements, which are correlated, than the models of [22, 24].

Another way to study the violation of SCHC is to measure the Φ angular distribution: $F(\Phi) \propto 1 - \varepsilon\ \cos 2\Phi\ (2r^1_{11} + r^1_{00}) + \sqrt{2\varepsilon(1+\varepsilon)}\cos\Phi\ (2r^5_{11} + r^5_{00})$, where ε is the polarisation parameter of the virtual photon. In the case of SCHC, this distribution is predicted to be uniform, the matrix elements r^1_{11}, r^1_{00}, r^5_{11} and r^5_{00} being zero.

The Φ distribution for the elastic ϕ meson production is presented in Fig. 6a. The distribution is corrected for the presence of ρ and ω backgrounds (hashed area). The result of the fit to the function $F(\Phi)$ is given as the full line and shows a clear $\cos\Phi$ dependence with a small $\cos 2\Phi$ modulation. The extracted values for the combination $(2r^5_{11} + r^5_{00})$ are presented in Fig. 6b for three bins in Q^2. The ρ and ω background subtraction in the Φ distribution reduces the value of the combination $(2r^5_{11} + r^5_{00})$ by 13 % (around half of the statistical error). In Fig. 6b, the effect of QED radiative corrections on the measurement of the combination $(2r^5_{11} + r^5_{00})$ was

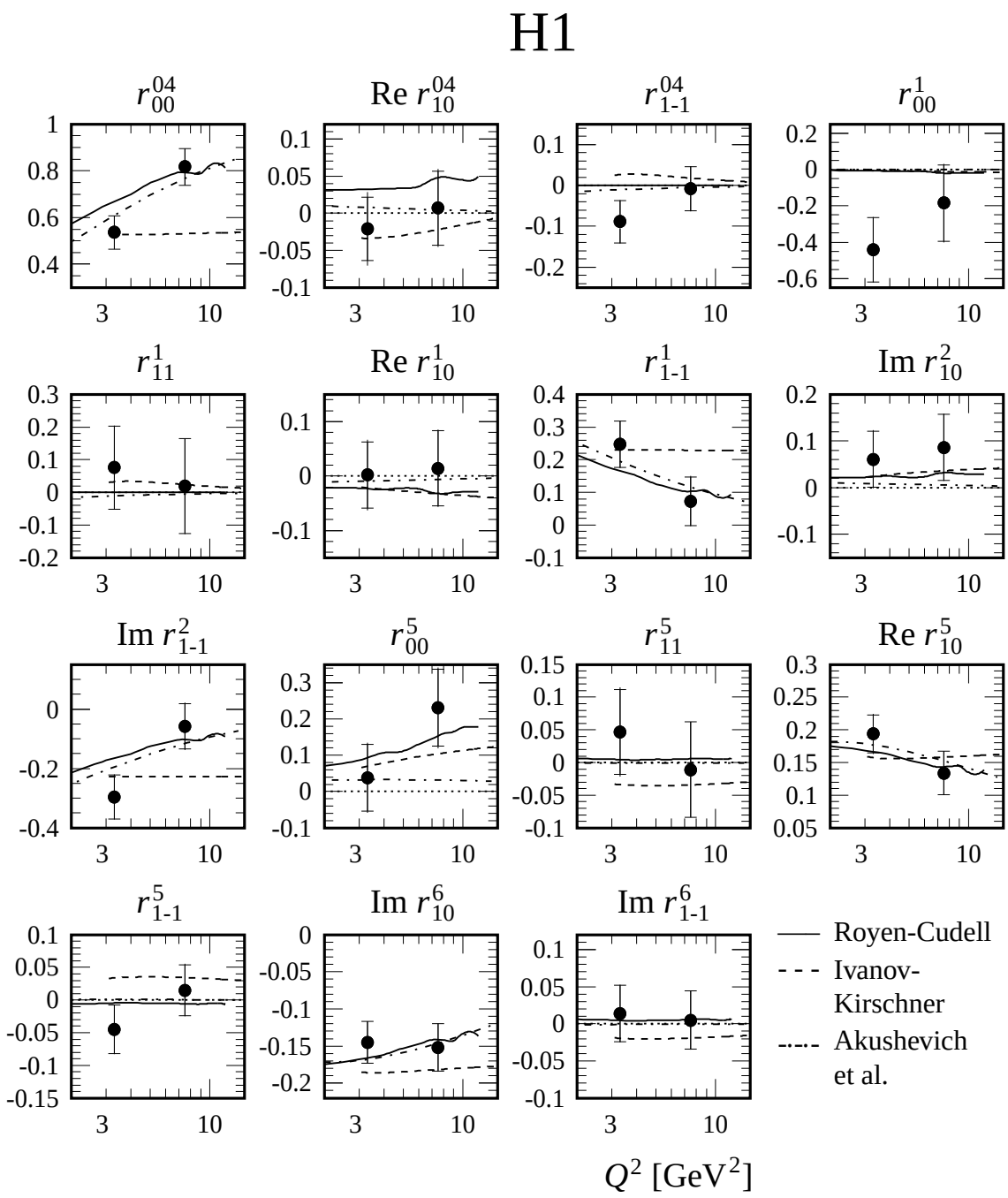

Figure 5: The full set of spin density matrix elements for elastic electroproduction of ϕ mesons, for two ranges of Q^2. The inner bars are statistical, the full error bars include the systematic errors added in quadrature. Where indicated the dotted lines show the expectation of zero for s-channel helicity conservation (SCHC). The five elements predicted to be non-zero under SCHC are r^{04}_{00}, r^{1}_{1-1}, Im r^{2}_{1-1}, Re r^{5}_{10} and Im r^{6}_{10}. The full, dashed and dash-dotted lines represent respectively predictions of the models of Royen and Cudell [22], Ivanov and Kirschner [23] and Akushevich, Ivanov and Nikolaev [24].

Q^2 (GeV^2)	$R = \sigma_L/\sigma_T$
2.0	$0.47\ ^{+0.26}_{-0.19}\ ^{+0.07}_{-0.06}$
2.9	$0.87\ ^{+0.38}_{-0.27}\ ^{+0.20}_{-0.06}$
4.5	$1.48\ ^{+0.82}_{-0.49}\ ^{+0.52}_{-0.09}$
8.6	$5.9\ ^{+5.6}_{-2.1}\ ^{+1.8}_{-0.5}$

Table 2: Ratio of the longitudinal to transverse cross sections for elastic ϕ meson production, for four Q^2 values. The first error represents the statistical error and the second the systematic error.

taken into account. This effect was estimated using the DIFFVM simulation including a HERACLES [20] interface, and reduces the observed value of the combination $(2r^5_{11} + r^5_{00})$ by 17 %. The combination $(2r^5_{11} + r^5_{00})$ obtained from the fit deviates significantly from the zero prediction of SCHC (a 5 σ effect). The values of the combination $(2r^5_{11} + r^5_{00})$ are similar to the ones obtained in case of elastic ρ meson production [1].

From the measurement of the spin density matrix elements, the ratio R of cross sections for ϕ meson production by longitudinal and transverse virtual photons can be extracted. As the SCHC violating amplitudes are small compared to the helicity conserving amplitudes, one can make[4] the SCHC approximation in order to estimate R, which is then obtained directly from the measurement of the matrix element r^{04}_{00} [1].

The Q^2 dependence of R is presented in Fig. 7a, together with other measurements performed under the SCHC approximation [6–8], see also table 2. It is observed that R rises steeply with Q^2, and that the longitudinal cross section dominates over the transverse cross section for $Q^2 \gtrsim 3$ GeV^2. The rise of R with Q^2 for ϕ meson production is slower than for the ρ meson [1]. However, when plotted as a function of Q^2/M_V^2, the ratio R appears to show a common dependence for different vector mesons [1–10], see Fig. 7b (for further details see ref. [18]).

6 Summary

The elastic electroproduction of ϕ mesons has been studied with the H1 detector in the kinematic range $1 < Q^2 < 15$ GeV^2 and $40 < W < 130$ GeV. The Q^2 dependence of the cross section is presented in the form of the ratio to the elastic ρ meson cross section. A significant rise of the ratio with Q^2 is observed. The elastic ϕ meson cross section is extracted using recent H1 results of elastic ρ meson production. A compilation of the elastic ρ, ω, ϕ, J/ψ and Υ meson cross sections, scaled by SU(5) factors, is presented as a function of (Q^2 + M_V^2). A common dependence is observed within experimental errors. The $|t|$ dependence of the elastic ϕ meson cross section is well described by an exponentially falling distribution. The full set of spin density matrix elements is measured in two Q^2 bins. Predictions based on perturbative QCD are compared to the measurements. The combination $(2r^5_{11} + r^5_{00})$ is extracted from the

[4]The effect of SCHC violation on the measurement of R is of the order of 3 %.

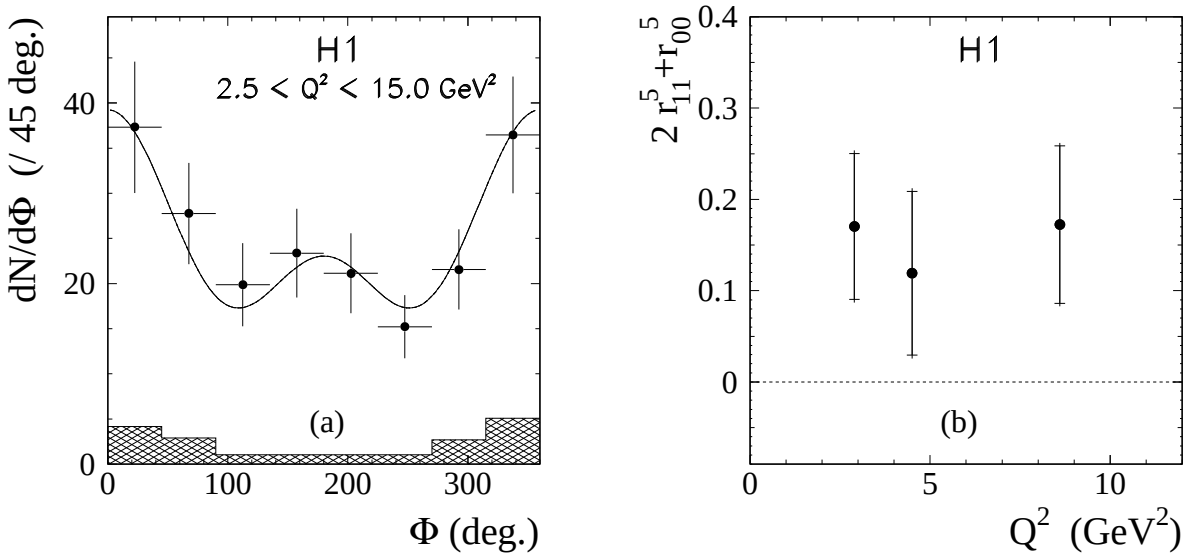

Figure 6: (a) Background corrected Φ angle distribution, the curve represents the result of a fit to $F(\Phi)$ (see text) and the hashed area the subtracted background, the errors on the data points are statistical only; (b) value of the combination of the matrix elements $(2r_{11}^5 + r_{00}^5)$ for three Q^2 bins, after background correction and QED radiative effects taken into account, the dotted line shows the zero prediction from SCHC, the inner error bars are statistical and the full error bars include the systematic errors added in quadrature.

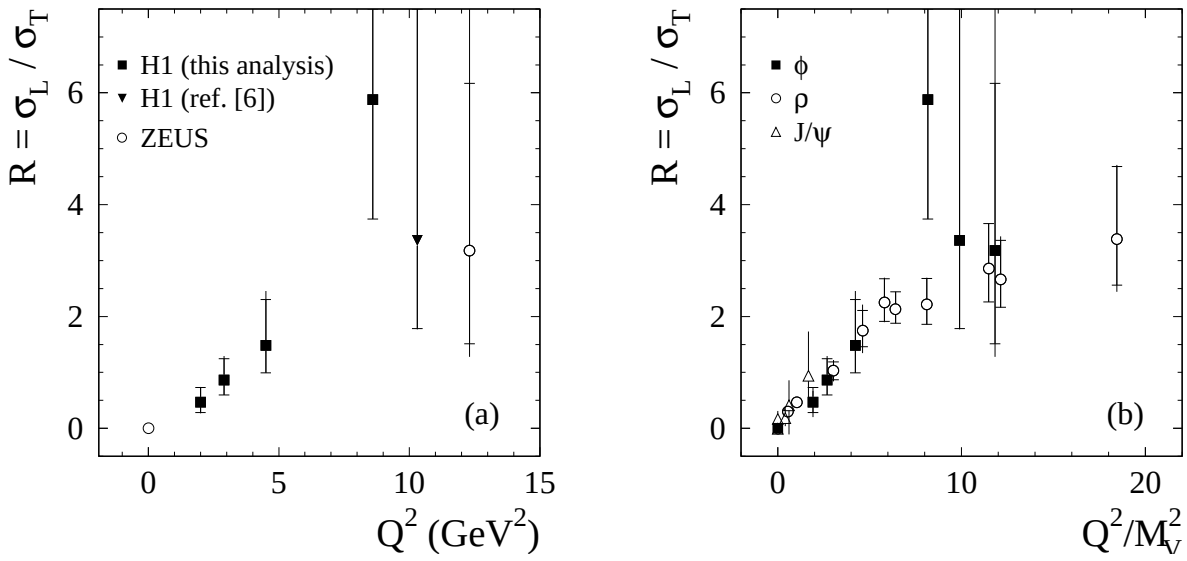

Figure 7: Ratio of the longitudinal to transverse cross sections for elastic ϕ meson production, as a function of Q^2 [6–8] (a) and for various vector mesons as a function of Q^2/M_V^2 (b) [1–10]. The inner error bars are statistical and the full error bars include the systematic errors added in quadrature.

Φ angle distribution and is observed to deviate from zero, which indicates a small but significant violation of the s-channel helicity conservation (SCHC) approximation. The ratio R of longitudinal to transverse ϕ meson production cross sections is observed to increase with Q^2. A common dependence for R as a function of Q^2/M_V^2 is observed for elastic ρ, ϕ and J/ψ meson production.

Acknowledgements

We are grateful to the HERA machine group whose outstanding efforts have made and continue to make this experiment possible. We thank the engineers and technicians for their work in constructing and now maintaining the H1 detector, our funding agencies for financial support, the DESY technical staff for continual assistance, and the DESY directorate for the hospitality which they extend to the non DESY members of the collaboration. We thank further I. Akushevich, J.-R. Cudell, D.Yu. Ivanov, N. Nikolaev and I. Royen for useful discussions and for providing us with their model predictions.

References

[1] C. Adloff et al., H1 Coll.,Eur. Phys. J. **C 13** (2000) 371.

[2] J. Breitweg et al., ZEUS Coll., Eur. Phys. J. **C 6** (1999) 603.

[3] C. Adloff et al., H1 Coll., Phys. Lett. **B 338** (1994) 507.

[4] C. Adloff et al., H1 Coll., Eur. Phys. J. **C 10** (1999) 373.

[5] J. Breitweg et al., ZEUS Coll., Z. Phys. **C 75** (1997) 215.

[6] C. Adloff et al., H1 Coll., Z. Phys. **C 75** (1997) 607.

[7] M. Derrick et al., ZEUS Coll., Phys. Lett. **B 377** (1996) 259.

[8] M. Derrick et al., ZEUS Coll., Phys. Lett. **B 380** (1996) 220.

[9] J. Breitweg et al., ZEUS Coll., Eur. Phys. J. **C 2** (1998) 247.

[10] J. Breitweg et al., ZEUS Coll., Z. Phys. **C 73** (1996) 73.

[11] C. Adloff et al., H1 Coll., *Elastic Photoproduction of J/ψ and Υ Mesons at HERA*, DESY-00-037, subm. to *Phys. Lett. B.*, hep-ex/0003020.

[12] J. Breitweg et al., ZEUS Coll., Phys. Lett. **B 437** (1998) 432.

[13] I. Abt et al., H1 Coll., Nucl. Instrum. Meth. **A 386** (1997) 310 and 348.

[14] R. Appuhn et al.,H1 SPACAL Group, Nucl. Instrum. Meth. **A 386** (1997) 397.

[15] S. Bentvelsen, J. Engelen and P. Kooijman, in: Proc. of the Workshop on *Physics at HERA*, ed. W. Buchmüller and G. Ingelman, Hamburg 1992, Vol. 1, p. 23;
K.C. Hoeger, ibid., p. 43.

[16] B. List, A. Mastroberardino (1999): DIFFVM: *A Monte Carlo generator for diffractive processes in ep scattering* in: A.T. Doyle, G. Grindhammer, G. Ingelman, H. Jung (eds): *Monte Carlo generators for HERA physics*, DESY-PROC-1999-02, page 396-404.

[17] L. Frankfurt, W. Koepf and M. Strikman, Phys. Rev. **D 54** (1996) 3194;
J. Nemchik et al., Z. Phys. **C 75** (1997) 71.

[18] B. Clerbaux, *Elastic production of vector mesons at HERA: study of the scale of the interaction and measurement of the helicity amplitudes*, IIHE-99-02 (ULB - Brussels), hep-ph/9908519.

[19] L. Frankfurt, M. McDermott and M. Strikman, JHEP **02** (1999) 002.

[20] A. Kwiatkowski, H.-J. Möhring and H. Spiesberger, Comput. Phys. Commun. **69** (1992) 155 and Proc. of the Workshop on Physics at HERA, ed. W. Buchmüller and G. Ingelman, Hamburg 1992, Vol. 3, p. 1294.

[21] K. Schilling and G. Wolf, Nucl. Phys. **B 61** (1973) 381.

[22] I. Royen and J.-R. Cudell, Nucl. Phys. **B 545** (1999) 505;
I. Royen, Nucl. Phys. Proc. Suppl. **79** (1999) 346;
I. Royen, ULG-PNT-00-1-IR (ULg - Liege), paper in preparation.

[23] D.Yu. Ivanov and R. Kirschner, Phys. Rev. **D 58** (1998) 114026.

[24] I. Ivanov and N. Nikolaev, JETP Lett. **69** (1999) 294;
I. Akushevich, I. Ivanov and N. Nikolaev, paper in preparation.